Energetics and Pattern Analysis of Crystals of Proflavine Deoxydinucleoside Phosphate Complex

Kwang S. Kim* and E. Clementi*†

Contribution from the National Foundation for Cancer Research, Bethesda, Maryland 20814, and IBM Corporation, IS & TG, Department D55, Poughkeepsie, New York 12602.
Received May 21, 1984

Abstract: Using the Metropolis Monte Carlo method with previously reported ab initio atom–atom pair interaction potentials, we have studied the networks of water molecules hydrating a 2:1 complex of proflavine and deoxycytidylyl-3′,5′-guanosine. Our results are discussed in terms of energetics and pattern analyses. There is good agreement with the X-ray patterns, especially for the simulated case of 61 and 66 water molecules per half unit cell, where we have assumed 10 to 15 extra water molecules not reported in X-ray analysis.

Recently, a number of X-ray studies have focused on drug complexes with dinucleoside monophosphates to understand the molecular mechanism of drug action on nucleic acids.[1-3] Analyses of the networks of water molecules in crystals of those complexes[2,3] are especially interesting in the viewpoint that theoretical studies by computer simulation can complement X-ray crystallography. We recall that by X-ray diffraction experiments the hydrogen positions of water molecules cannot be found. Secondly, if water molecules in crystals are mobile or disordered, there are difficulties in diffraction experiments to determine the correct positions, even for the oxygen atoms. Therefore, it is of significance to compare theoretical and experimental conclusions and to propose reasonable interpretations if discrepancies are encountered.

Previously, we have reported[4] a preliminarily simulation on the network of water molecules in a crystal of a deoxydinucleoside–proflavine complex, comparing it with a diffraction analysis by Neidle, Berman, and Shieh.[2] Almost at the same time, Beveridge et al.[5] reported a related simulation study; by assuming the same number of water molecules as reported in the X-ray experiment, they simulated positions for the oxygen atoms and found them to be in agreement with the X-ray data within 40 to 60%. As it is expected from our preliminary report,[4] communications with Neidle and Berman,[6] and X-ray experiments on a second crystal,[2] some extra water molecules (in addition to the reported 50 water molecules per half unit cell) are likely to be present. Therefore, in order to determine the correct number of water molecules in the crystal, we have investigated the effects of varying the number of water molecules (NW) from 50 to 82 per half unit cell, comparing the energies and patterns obtained from Monte Carlo (MC) simulations.

From the X-ray study on the crystal,[2] the two dinucleoside phosphate strands form self-complementary duplexes with Watson–Crick hydrogen bonds in the 2:2 complex of proflavine:deoxycytidylyl-3′,5′-guanosine, i.e., Pf:d(CpG). One proflavine (Pf) is asymmetrically intercalated between the base pairs (C–G), and the other is stacked above them as shown in Figure 1. The crystal has a space group $P2_12_12$. A unit cell consists of 4 asymmetrical units arranged in such a way as to define major and minor grooves. The length, width, and height of a unit cell are x = 32.991 Å, y = 21.995 Å, and z = 13.509 Å, respectively.

In the X-ray data, the water molecules are connected continuously from M (a major groove) to M′ (another major groove) and from m (a minor groove) to m′ (another minor groove) along the z axis. In addition, the water molecules are connected from M to m (or vice versa) along the x axis. However, they are not connected between M and m along the y axis (i.e., the nearest ones are more than 5.5 Å apart according to the X-ray data). Therefore, for the water–water interactions in our MC simulation, we can consider a half unit cell as a primitive cell for the water molecules, while utilizing suitable symmetry operations with these water molecules for a periodic boundary condition. This one-half unit cell corresponds to the portion inside the rectangular box in Figure 1. If a primitive cell is reduced to a quarter unit cell as in the solute of the crystal, some water molecules are near the symmetry axis, and thus, the thermal statistical effect for these molecules cannot be properly considered. Also, such symmetry constraint on water would be, in general, too strong and artificial for real complex-crystal systems. It should be noted that *the space group of the molecular complex alone (crystal solute) is not necessarily the same as the space group of the hydrated crystal.* Furthermore, if there is disordered water, then strictly speaking, there is no symmetry in the hydrated crystal.

In our MC simulations, the d(CPG) and Pf species are assumed rigid at the positions given from the X-ray data; the attached hydrogen atoms for these species have been added with the standard bond lengths and angles. The boundary condition is not limited to a volume which would include only a single unit cell, as is often done for neutral solutes. The presence of the negatively charged groups (PO_4^-) and of the positively charged proflavines (Pf^+) *complels one to consider a much larger volume in order to take into account the long-range ionic field which extends further than the dimension of a unit cell.* If either d(CpG) or Pf would be partitioned into more than two fragments, then the water molecules would experience a strong monopole electric field (an artifact of the partitioning) rather than a dipole electric field. Therefore, in our MC simulation we consider three sets of the 16 asymmetric unit cells of Figure 1, stacked in three layers along the z axis. For the water molecules in the major groove, the left 12 × 3 asymmetric unit cells are considered as the periodic boundary conditions, while for the water molecules in the minor groove, the right 12 × 3 asymmetric unit cells are used. In this way, the boundary condition is imposed in a very symmetrical manner as it should be, and the discontinuity of the potential near the border of major and minor grooves is really negligible in our MC study.

† Present Address: IBM Corporation, Department 48B, Mail Station 428, P.O. Box 100, Neighborhood Road, Kingston, NY 12401.

(1) H. M. Sobell, C. C. Tasal, S. C. Jain, and Gilbert, *J. Mol. Biol.*, **114**, 333 (1977); H. M. Berman, S. Neidle, and R. K. Stodola, *Proc. Natl. Acad. Sci. U.S.A.*, **75**, 828 (1978); S. Neidle, *Prog. Med. Chem.*, **16**, 151 (1979); S. Neidle, G. Talylor, M. Sanderson, H. S. Shieh, and H. M. Berman, *Nucleic Acids Res.*, *5*, 4417 (1978); E. Westhof, S. T. Rao, M. Sundarlingam, *J. Mol. Biol.*, **142**, 331 (1980); E. Westhof and M. Sundarlingam, *Proc. Natl. Acad. Sci. U.S.A.*, **77**, 1852 (1980).

(2) H. S. Shieh, H. M. Berman, M. Dabrow, and S. Neidle, *Nucleic Acids Res.*, **8**, 85 (1980); S. Neidle, H. M. Berman, H. S. Shieh, *Nature (London)* **288**, 129 (1981).

(3) P. Swaminathan, E. Westhof, and M. Sundarlingam, *Acta Crystallogr., Sect. B, B38*, 515 (1982).

(4) K. S. Kim, G. Corongiu, and E. Clementi, *J. Biomolecular Struct. Dynamics*, 1, 263 (1983).

(5) M. Mezel, D. L. Beveridge, H. M. Berman, J. M. Goodfellow, J. L. Finney, and S. Neidle, *J. Biomolecular Struct. Dynamics*, **1**, 286 (1983).

(6) Private communication from S. Neidle and H. M. Berman to K.S.K.

0002-7863/85/1507-0227$01.50/0

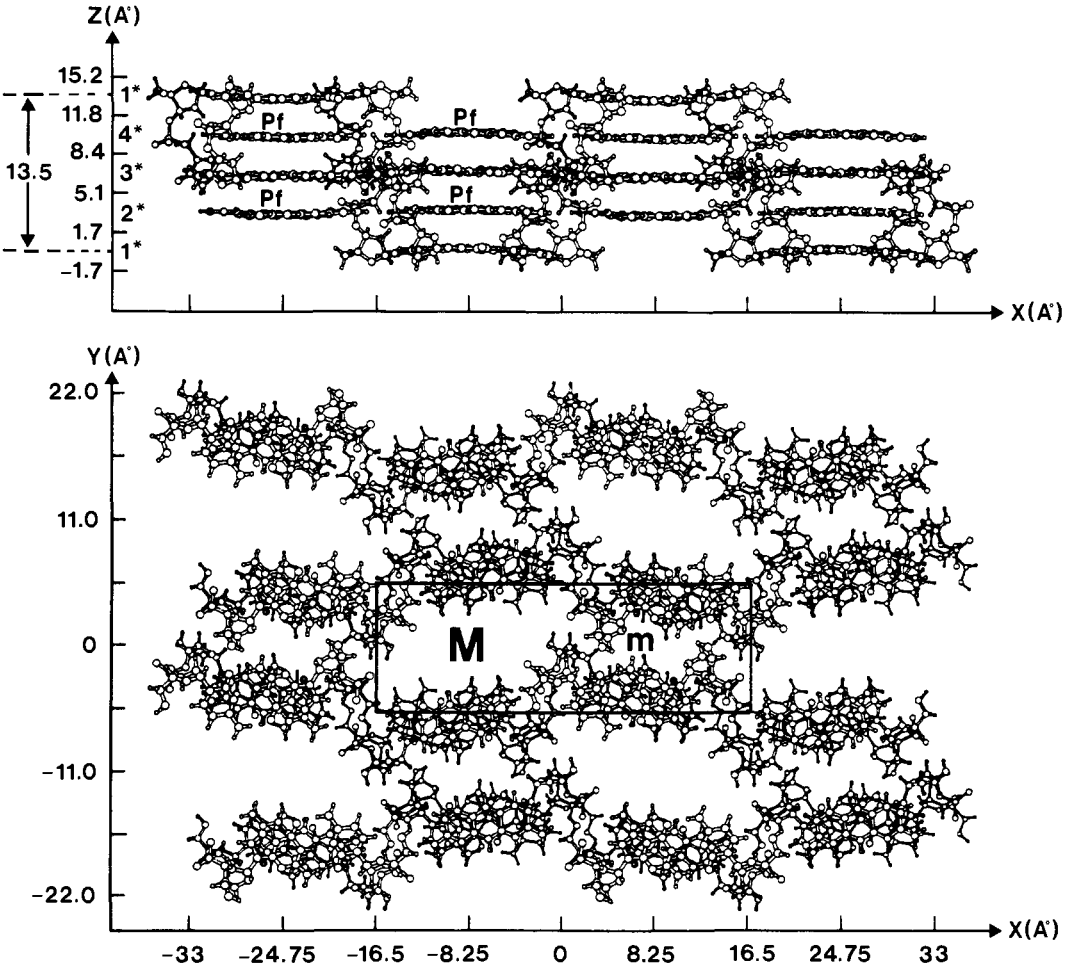

Figure 1. Projection of 16 asymmetric unit cells with the $P2_12_12$ space group symmetry onto the x–z (top) and x–y (bottom) planes. Our MC simulation considers three such sets, stacked in three layers along the z axis. An asterisk indicates that for the analysis, the crystal is partitioned into 4 portions, denoted as 1, 2, 3, and 4. Note the preriodicity along the z axis with the Pf stacks in subvolumes 2 and 4 and the G–C stacks in subvolumes 1 and 3.

In our MC simulation (which follows Metropolis, et al.[7]) we have used the previously reported ab initio atom–atom pair interaction potentials[4,8,9] between a water molecule and a sugar, a phosphate, G and C bases, a proflavine cation, and another water molecule. All our computer simulations have been done at 0 °C, since we previously[4] indicated that there were no significant differences between the hydration patterns computed at two different temperatures of 0 and 27 °C.

In order to facilitate our analysis, the crystal is partitioned into 4 subvolumes denoted by 1, 2, 3, and 4, as seen in the x–z projection (Figure 1, top). The periodicity along the z axis can be observed from the subvolumes in the x–z projection. Subvolumes 2 and 4 show Pf stacks, while subvolumes 1 and 3 show C–G stacks.

MC Simulations

A. Comparison of X-ray Data with Simulation Results for NW = 50. Neidle et al.[2] proposed the pattern given in Figure 2a for the network of water molecules in the crystal; hydrogen bonding is assumed if the distance between two oxygen atoms is less than 3.5 Å. As is known, this assumption is rather crude and possibly incorrect unless the interaction energy between the two corresponding water molecules is attractive; this can be the case when a hydrogen atom of one water molecule is aligned with the oxygen of the other water molecule. Once the oxygen positions for the water molecules are given, it is easy to determine the hydrogen positions by MC simulations. By first assuming the oxygen positions to be those given by the X-ray data and keeping such positions fixed in an MC simulation, the corresponding hydrogen positions are allowed to rotate freely. The hydrogen positions are then ensemble averaged for the final 200 000 MC steps after a reasonable equilibration. Figure 2 shows the simulated result which is denoted as NW = 50X to distinguish it from the simulation denoted as NW = 50, where the oxygen positions can also move freely (see below).

Figure 2b shows the simulated hydrogen-bonding structures. The periodicity is self-evident. The x–z and x–y projections of the 50 water molecules per half unit cell are shown in Figure 2, parts c and d, respectively. To facilitate the hydration analysis, the water molecules are numbered from 1 to 50. Each odd number is related by symmetry to the next highest even number, except that 49 and 50 are unique and have no symmetrically related number.

The bottom four insets in Figure 2 show the hydrated structures in the four subvolumes 1, 2, 3, and 4 (cf. the x–z projection in Figure 1). Each inset shows the detailed analysis of the hydration relating each numbered water molecule to the hydration sites of the complex (solute). Note that phosphate is denoted by P, proflavine by F, cytosine by C, and guanine by G. The oxygen and nitrogen atoms of the complex are darkened in order to more easily recognize hydrophilic sites. Note also that atoms of higher z value are larger in size than those with lower z value. From Figure 2 one can see that the hydrogen orientations lose symmetry,

(7) N. Metropolis, A. W. Rosenbluth, M. N. Rosenbluth, A. H. Teller, and E. Teller, *J. Chem. Phys.*, **21**, 1078 (1953).
(8) O. Matsuoka, E. Clementi, and M. Yoshimine, *J. Chem. Phys.*, **64**, 1351 (1976).
(9) G. Corongiu, and E. Clementi, *Gazz. Chim. Ital.* **108** (506), 273 (1978); E. Clementi, G. Corongiu, and F. Lelj, *J. Chem. Phys.*, **70**, 3726 (1979); R. Scordamaglia, F. Cavallone, and E. Clementi, *J. Am. Chem. Soc.*, **99**, 5545 (1977); G. Corongiu and E. Clementi, *Int. J. Quantum Chem.*, **9**, 213 (1982).

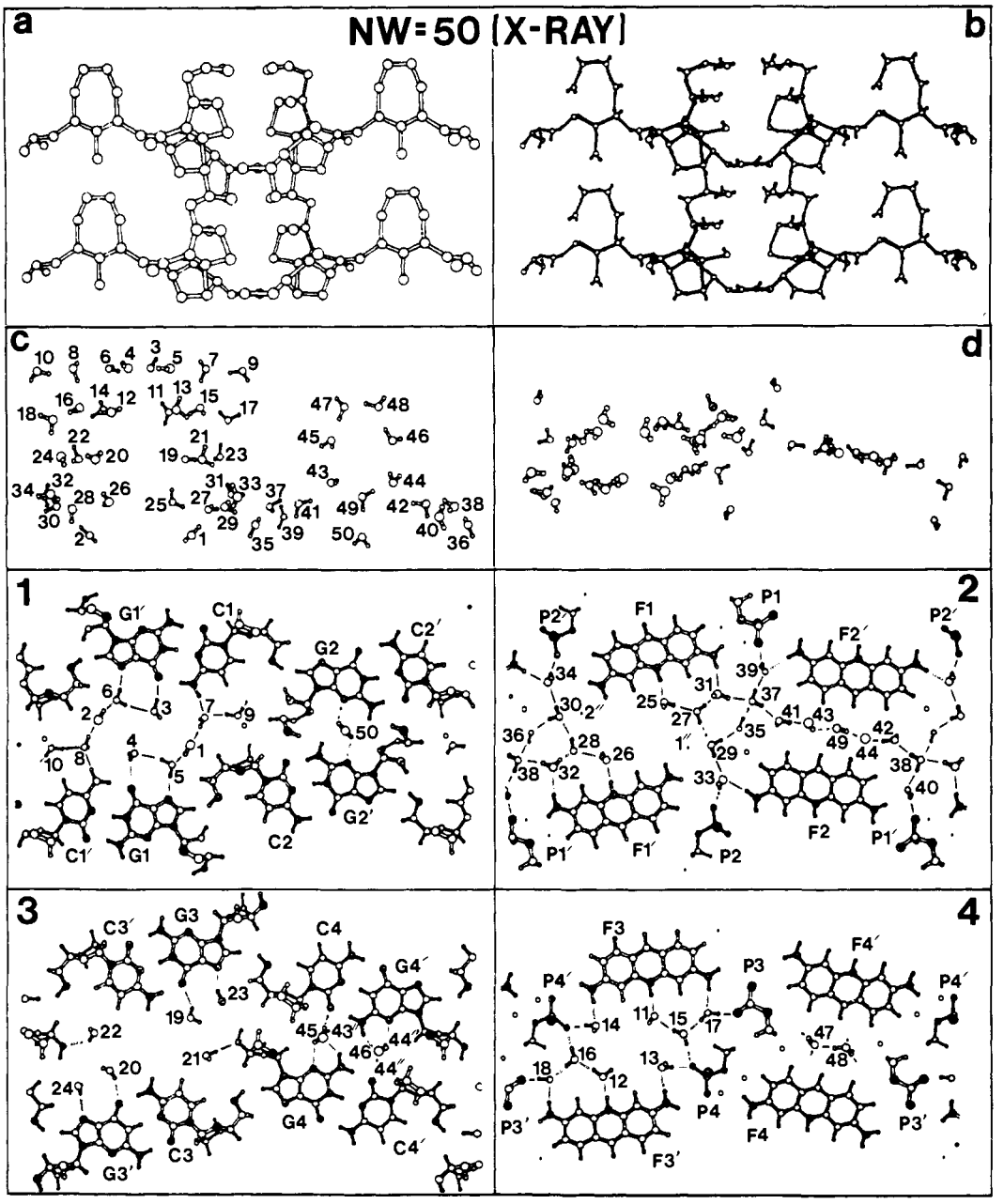

Figure 2. Hydrogen bonding patterns for a simulation with NW = 50X. "a" is the x–z projection of the oxygen atoms of the water molecules showing the possible hydrogen bonding (as given in the X-ray data); "b" is the networks of the water molecules; "c" and "d" are the x–z and x–y projections of water molecules, respectively. The bottom four insets show x–y projections of the subvolumes 1–4 corresponding to the numbers in the top inset of Figure 1. The darkened circles are either oxygen or nitrogen atoms, showing hydrophilicity. The water molecules are numbered from 1 to 50 (see text).

especially in the vicinity of the symmetry axis. This will necessarily make the solutes partially disordered near the symmetry axis, as mentioned in the X-ray experiment.[2] We also find that water molecules, 1, 27, 35, 37, and 49 (and 2, 28, 36, and 38), are not bound to the solute but are weakly bound to neighboring water molecules.

Having discussed the NW = 50X case (where the oxygen positions are kept frozen but the hydrogens can rotate freely), let us consider the NW = 50 case (where the oxygens can also move freely in addition to the hydrogens which can rotate). The results for the NW = 50 are presented in Figure 3 in a fashion similar to that in Figure 2 for the NW = 50X case. The two figures show similar patterns. Most of the water molecules in Figure 3 are *almost* at the same positions as the water molecules in Figure 2. Let us assume that the conclusions drawn from the X-ray data are exact and complete. In this case, our simulation appears to be in limited but reasonable agreement. The most conspicuous difference in the NW = 50 case is that several water molecules (5, 6, 28, 35, 36) disappeared from the X-ray positions and *migrated* into different positions (designated as 52, 57, 58, 59, 64). Water molecule 5 (and its symmetrically equivalent partner 6) which hydrates G1/N7 (and G1′/N7, by symmetry) for NW = 50X (Figure 2.1) is no longer present in the NW = 50 case (Figure 3.1). On the other hand, molecule 57 (and correspondingly molecule 58) hydrates C3/NH_2 (and correspondingly C3′/NH_2) for the NW = 50 simulation (Figure 3.3), while it is absent in the NW = 50X simulation (Figure 2.3). Also note that molecule 35 (and molecule 36) disappeared in the NW = 50X case. However, for the pair of molecules 27 and 28, while molecule 28 disappears, molecule 27 does not disappear but moves far away from the corresponding X-ray position. The same situation occurs for molecule 1 (and molecule 2). We recall that molecules 1, 27, and 35 (and molecules 2, 28, and 36) were not bound to the solutes for the case of NW = 50X.

Let us stress that if 50 is not the correct number of water molecules, but only a faction of it, when those *weakly* bound water

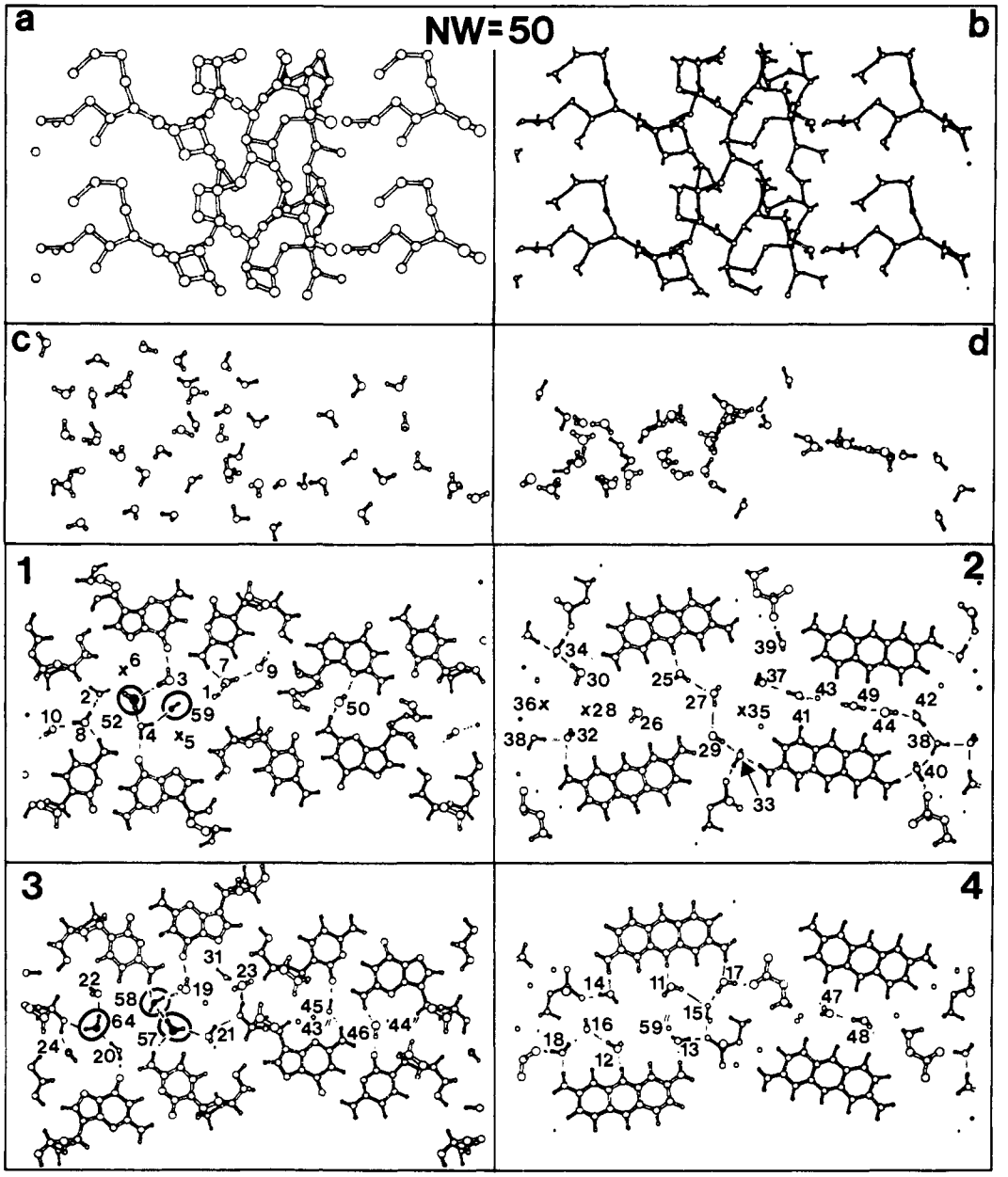

Figure 3. Hydrogen bonding patterns for the simulation with NW = 50 (cf. Figure 2; see text).

molecules originally determined in the diffraction study will tend to migrate toward energetically more favorable positions, if available, thus deviating from the positions determined from the X-ray data. In fact, for NW = 50, several such water molecules migrated from the positions toward the vacant region in the major groove; this can be easily noticed by comparing Figure 3 with Figure 2 (especially for inset "d").

Therefore, we may hypothesize that there must be water molecules undetected by the X-ray experiment (likely due to disorder and mobility of the water molecules). This supposition is born out by the fact that for NW = 50 in Figure 3, some hydration sites (for example, NH_2 of Pf^+ and N7 of G) are not hydrated at all, and even for NW = 50X in Figure 2 a few sites (for example, NH_2 of Pf and NH_2 of G) are not hydrated either. This supposition is again partially supported by Neidle and Berman,[6] who have mentioned that 54 to 58 water molecules could have been present in the diffraction experiment. With this in mind, we have carried out MC simulations from NW = 50 up to NW = 82; for each simulation we have studied the energetics and compared the resulting patterns with the X-ray data.

B. Energetics. In this section we shall consider the overall energetic effects from our MC simulation results (NW = 50, 57, 61, 66, 69, 72, 77, and 82). In Figure 4a we show the convergency behavior for each NW simulation. The number of MC steps are about 800 000, except for the NW = 82 case for which only 500 000 steps are used. For the analyses, we chose 200 000 steps as our samples except for the NW = 82 case for which only the last 100 000 steps were used.

In Figure 4b the total energy per mole of water is shown for each NW case. As NW increases about 70, the curve becomes rather steep, which may imply the beginning of a strong pressure buildup inside the crystal. We should mention that for NW = 87 there was a drastic increase in the slope of the curve.

In Figure 4d, we show the thermoenergetics for the system comprised of a crystal and water, where ΔE is the internal energy change at T = 0 °C. From an MC simulation at 0 °C with a weight density of water equal to 1, the internal energy E(W) of pure bulk water is −37.7 kJ/mol. When the crystal is grown with enough water at constant temperature T and pressure P, the total change in Gibbs free energy is $\Delta G = G(\text{Tot}) - G(\text{St}) - G(\text{W})$, where St, W, and Tot denote solute, water, and the hydrated crystal, respectively. Let us consider $\Delta G = \Delta E - T\Delta S + P\Delta V$ at constant T and P. The temperature of our simulated system is 0 °C, and the pressure is not expected to change drastically for NW ≤ 70. As long as the pressure buildup is not too strong inside the crystal, the $P\Delta V$ term is negligible compared with the internal

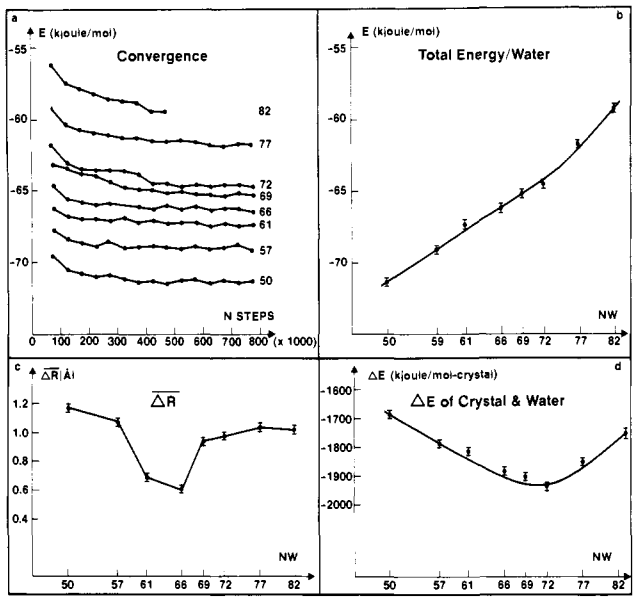

Figure 4. Convergence, total energy per mole of water, average distance deviation ($\overline{\Delta R}$) (see Figure 5 for details), and internal energy change (ΔE) of the crystal–water system.

energy change, ΔE. However, if the phase transition between the free water and hydrating water is considered, the $T\Delta S$ term is not negligible, though it is still not comparable to ΔE. Note that we are not interested in the absolute magnitude of ΔG, but only in which NW value gives the minimum for ΔG. Since for all our simulations the water molecules are already crystalline, ΔS values will not be significantly different for each NW value. The only differences are due to small variations in the respective crystal hydration. Furthermore, from Figure 4d it can be seen that the energy change with respect to NW is very large relative to the latent heat of water. Therefore, we would like to argue that inside the crystal the entropy contribution should not change drastically, unless P changes drastically. And the change of ΔG with respect to NW can be approximated by the change of ΔE, unless NW is larger than 70. Accordingly, Figure 4d shows that the case of NW = 70 would be the most thermoenergetically favorable one for the hydrated crystal system.

However, our simulated energies are very sensitive to the assumed pair potentials. Since the three-body correction[10] and other corrections have been neglected in the water-water interaction, our potentials are presently not well enough refined for these purposes; for the water–solute case the potentials are even rougher. Therefore, the values of ΔE are not two reliable; our result for the most energetically favorable case may be NW = 70 ± 10.

A detailed summary of the energetics for each NW is given in Table I, including the total interaction energy E(Tot), interaction energy between water and solute E(St,W), interaction energy between water and water E(W,W), and internal energy change of the solute–water system due to the solvation ΔE(Solv). Here, E(Tot) = E(St,W) + E(W,W) with units of kJ/(mol of water, and ΔE(Solv) = E(Tot) − E(St) − E(W), where the internal energy of anhydrated crystal E(St) is chosen to be "0" as the reference point and E(W) is −37.7 kJ/mol taken from the MC simulation. Therefore, the solvation energy for one-half unit cell can be represented as ΔE(Solv) = NW(E(Tot) − E(W)), where the units of ΔE(Solv) are kJ/(one-half mole unit cell of crystal). Note that if we would have carried out the MC simulation with a crystal system consisting of only one unit cell (our system consists of 12 unit cells), the energetics would be notably different; the long-range effects of the ions (positively charged phosphates and negatively charged proflavines) would have been underestimated.

C. **Pattern Analysis.** The X-ray diffraction patterns of molecular crystals are generally limited to atoms or molecules relatively fixed at a given site. In addition, when symmetry constraints are imposed on the scattering intensities, the diffraction patterns are limited to those atoms or molecules belonging to a given point group; in this way "disordered" atoms or molecules are neglected. These limitations are not present in our MC analysis; thus, MC simulations *complement* diffraction studies, a most important aspect of our work.

(10) E. Clementi and G. Corongiu, IBM IS & TG POK-20 (1983).

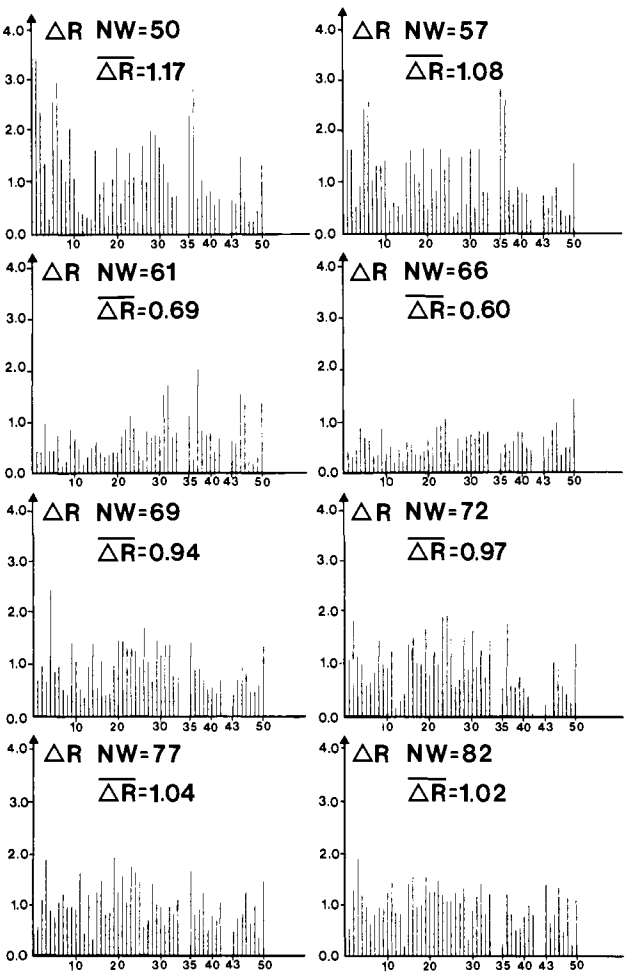

Figure 5. Distances from the X-ray oxygen positions to the nearest simulated ones (in Å). While for the X-ray data 40 molecules are in the major groove and 10 molecules in the minor groove, we chose 34 in the major, 8 at the border (6 from major and 2 from minor), and 8 in the minor groove.

Whereas the energetics are very sensitive to given pair potentials, the pattern analysis is rather insensitive to those potentials, since water molecules have finite volume and well-defined shape (namely the steric factor). Even if we consider the extreme case of hard-core potentials, the pattern would retain much of its character. Indeed, we have computed the volume available to water molecules within the crystal (for a half unit cell) by measuring the available volume in the several equipartitioned subvolumes composing the half unit cell and also by computing the available volume with use of the hard-core potentials with the MC method. Both methods yielded a volume of 65 ± 10 water molecules at a weight density of 1.

For the pattern analysis, let us first compare the average distance deviation ($\overline{\Delta R}$) from the X-ray oxygen positions to the nearest simulated oxygen position (see Figure 4c). The detailed water-by-water analysis is shown in Figure 5. The most favorable case is found to be 66 water molecules (possibly 61 ≤ NW ≤ 66).

Considering that the maximum X-ray resolution was 0.83 Å and that the average resolution was 0.62 Å, the deviation of $\overline{\Delta R}$ = 0.60 Å is within the range of experimental error. Thus, by assuming that a few water molecules could have been missed by the X-ray analysis, the NW = 66 case (and the NW = 61) is in notable agreement with the X-ray data.

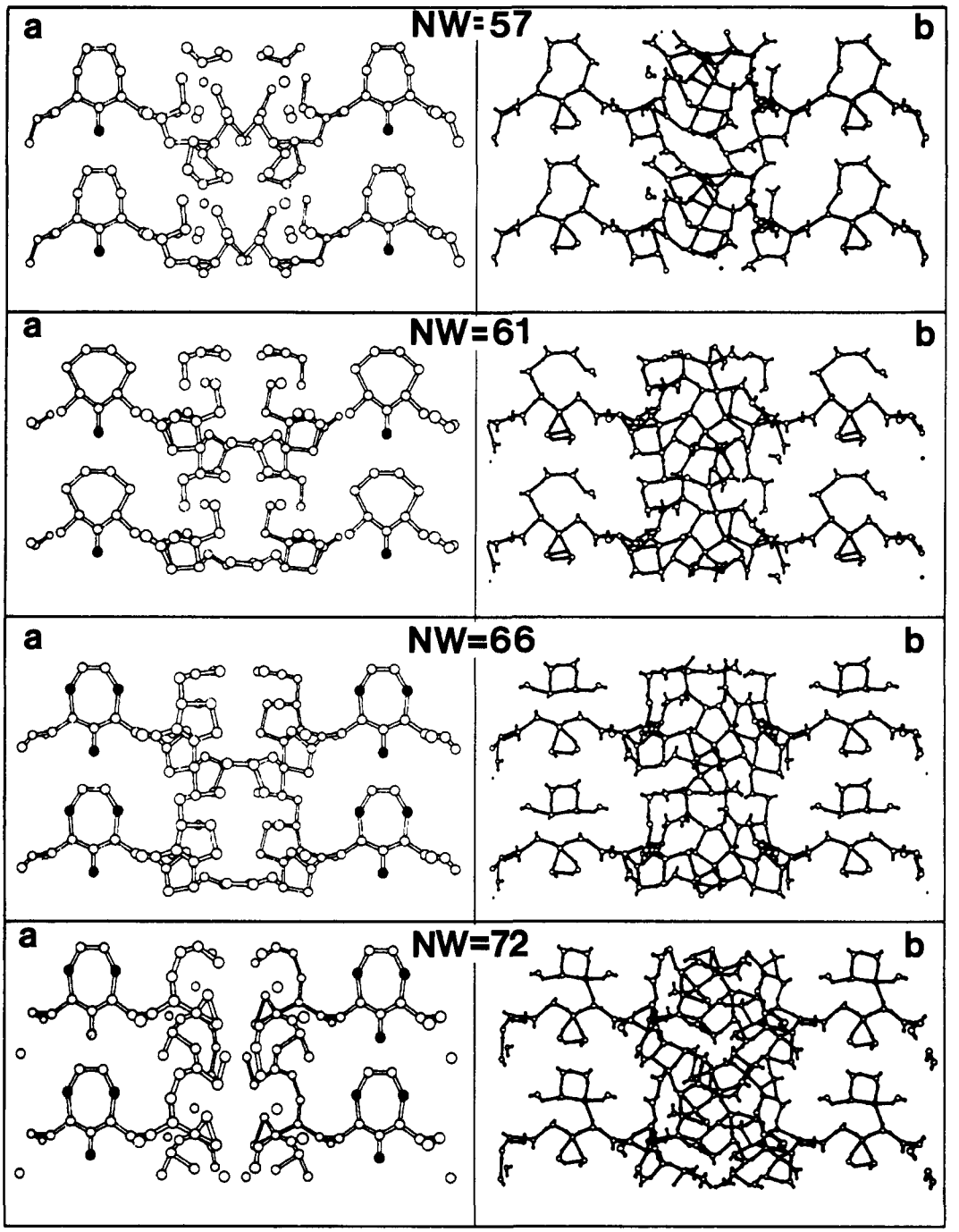

Figure 6. Hydrogen-bonding patterns (x–z projections) for the simulations of NW = 57, 61, 66, and 72 (cf. Figure 2, parts a and b). Insets "a" represent the 50 oxygen positions obtained by averaging the symmetrically conjugate ones which best fit with one-to-one correspondence to the X-ray data. If the possibility for hydrogen bonding exists, the oxygen atoms are connected. The filled circles denote the average positions of double occupancies. Insets "b" represent the networks of all the water molecules in each simulation.

For NW = 50 in Figure 5, four water molecules (2, 5, 9, 35), have ΔR larger than 2 Å and three (1, 6, 36) larger than 3 Å. This means that one can insert an extra water molecule in a vacant space with energetically acceptable distances among the water molecules and between the water molecules and the atoms of the solute. Indeed, for the case NW = 50, there is enough space to put extra water molecules into the seven positions missed by the X-ray. Likewise, from the NW = 57 case we learn that at least four water molecules (5, 6, 35, 36) again migrated to other energetically more favorable positions.

For the NW = 61 case, ΔR's are small except for six water molecules which deviate somewhat from the X-ray positions. However, the deviation of the sixth (50) water molecule may be explained. We note that this molecule shows a deviation of 1.3–1.5 Å in our eight simulation cases (see Figure 5). In particular, for NW = 50, the 50th water molecule shifted to the left (see Figures 2 and 3) leaving a possible hydration site on the right side. If we assume that the X-ray position for the 50th molecule corresponds to the average value of the 50th position and its symmetrically conjugate position, then the 50th water molecule nicely matches the experimental data in each simulation case (see Figure 6).

With such an argument, the study with NW = 66 in Figure 5 shows essentially no discrepancy from the experiment. When we add more water molecules in addition to 66 water molecules, then $\overline{\Delta R}$ increases. However, it is clear that by packing more and more water, the deviation $\overline{\Delta R}$ would eventually decrease. For these cases, the energies are totally unfavorable; thus, we do not need to consider cases where NW $\geq$ 82.

Table I. Total Energies E(Tot), Interaction Energies between Solute and Water E(St,W), Interaction Energies between Water and Water E(W,W), Energy Change of Crystal and Water System ΔE(Solv), Standard Deviation of Oxygen (STO) and Hydrogen (STH) Positions, Average Distance R(OO′) between the Nearest Oxygens; Average Distance Deviation ($\overline{\Delta R}$) from X-ray Data (Cf. Figure 5), and Number of Water Molecules in Minor/Major Grooves (m/M)[a]

	E(Tot)	E(St,W)	E(W,W)	ΔE(Solv)	STO	STH	R(OO′)	$\overline{\Delta R}$	m/M
50X	−60.2	−41.1	−19.1	−1125	0.0	0.36	2.79	0.0	10/40
50	−71.4	−52.1	−19.3	−1685	0.39	0.43	2.90	1.17	10/40
57	−69.0	−47.8	−21.2	−1784	0.44	0.49	2.86	1.08	11/46
61	−67.4	−45.5	−21.9	−1812	0.40	0.46	2.85	0.69	11/50
66	−66.3	−44.9	−21.4	−1888	0.36	0.43	2.83	0.60	13/53
69	−65.3	−43.4	−21.9	−1904	0.34	0.38	2.81	0.94	13/56
72	−64.7	−43.0	−21.7	−1934	0.32	0.37	2.81	0.97	13/59
77	−61.8	−40.7	−21.1	−1848	0.30	0.35	2.78	1.04	13/64
82	−59.3	−38.2	−21.1	−1771	0.27	0.31	2.78	1.02	14/68

[a] Energies are in kJ per mol of water except that ΔE(Solv) is in kJ per mol of one-half unit cell of crystal, and distances are in Å.

Our simulation results are shown in Figure 6 for NW = 57, 61, 66, and 72. Four simulated hydrogen bonding patterns are shown in insets "b" of Figure 6 and should be compared with those in Figures 2b and 3b. However, since the full patterns are rather complicated, we will consider only those water molecules which are reported in the X-ray analyses.

In addition, we also take into account the statistical disordering of water molecules. For example, in each "a" inset (and "b") of Figures 2, 3, and 6, we presented only one hydrogen-bonding pattern for each simulation, realizing there is a second symmetrically conjugate pattern with the same energy due to the symmetric boundary condition. If we take into account the fact that the interaction energy between the water molecules in a major groove and the water molecules in a minor groove is very weak, each major groove can be in either state of the two conjugate patterns without any noticeable energy change; the same holds for each minor groove. Of course, the pattern inside each groove is *not symmetric* due to the peculiar networks of hydrogen bonding.

We recall that, in general, the X-ray experiment cannot distinguish between the two symmetrically conjugate patterns because of its limited resolution, and thus, it will give only the average value of the two patterns. Therefore, in order to compare with the proposed X-ray structure, we also need to to average the symmetrically corresponding positions of the oxygen atoms. If we assume that the X-ray analysis cannot resolve mobile water molecules (namely thermally disordered), these mobile water molecules also need to be eliminated from our simulation results for the comparison. Therefore, for each analysis we chose to compare the 50 water molecules which best fit with the X-ray data. These are shown in the "a" insets of Figure 6. In these figures, the darkened circles denote averaged positions resulting from double occupancies, which are reported as single occupancies in the X-ray work. One such case is water molecule 50 of the X-ray data. Another one is molecule 45 of the X-ray data (cf. NW = 66 and 72 of Figure 6).

Let us consider the simulated oxygen–oxygen pattern for NW = 66 shown in Figure 6a. The match of the X-ray (Figure 2a) to the MC simulation is impressive. On the other hand, for the NW = 50 case we could not find the symmetrically corresponding positions for several water molecules due to their migration into the empty space in the major groove; for this reason we did not average (see Figure 3a).

In Table I, we show the standard deviation of the oxygen (STO) and hydrogen (STH) positions. As NW increases, the standard deviation tends to be reduced, except for the simulations with NW = 50 to 57. This result may be rationalized by the observation that in the NW = 50 case there is rather little water, and thus, most hydration sites strongly bind these water molecules, while for NW = 57 there are some mobile water molecules due to water–water interactions.

We also report, in Table I, the average distance R(OO′) between one oxygen and its nearest oxygen atom. The value for NW = 50 is 2.90 Å. This value seems to be somewhat large compared with the value of 2.85 Å for pure bulk water[11] and 2.80 Å for ice at 0 °C and 1 atm. For NW = 77, the value of 2.78 Å is somewhat small. The values of R(OO′) for $57 \leq NW \leq 66$ have more reliable values and are between 2.83 and 2.86 Å.

Discussion

Comparing the MC simulation with the X-ray data, we find good agreement; however, in our MC simulation we must assume some extra water molecules that are not reported in the X-ray analysis. Our simulation results suggest about 70 water molecules per half unit cell by the thermoenergetical study and about 61–66 water molecules by the "pattern" comparison. These results must be compared to the X-ray conclusion, which shows only 50 water molecules, or possibly up to 54 or 58 water molecules.[6] Therefore, let us survey a few factors which could be sources of errors in our analysis.

First, we are using the MCY potential[8] for water–water interactions. This potential has been rather well tested and has often given good agreement with experiments.[11] However, it is well-known that its interaction energy (−38 kJ/mol at 300 K) for pure bulk water is somewhat smaller than the experimental[12] value (−42 kJ/mol at 300 K). With use of the experimental interaction energy of pure bulk water (instead of the computed one) as the reference energy, the number of water molecules in our study could be reduced. However, the energy comparison of the system of isolated solute and isolated water with the system of the hydrated crystal must be studied in a consistent manner with the same theoretical methods; otherwise a reduction in the number of water molecules by using experimental values would be an artifact.

Second, if we consider the many-body correction for each system, the water–water interaction energy will be increased in both systems and so will the solute–water interaction energy. Therefore, the many-body correction would not significantly change the number of water molecules due to the cancelling-out effect.

Third, the interaction energy of the hydrated crystal was calculated with a minimal basis set, but without the counterpoise correction.[13] Since the counterpoise correction can be rather important when a minimal basis set is used, our interaction energy of the hydrated crystal could be overestimated. By assuming a reduction of the interaction energy by 50%, the optimal number of water molecules can be reduced by about 5. This would bring all the analyses in agreement with a value of NW between 60 and 66.

Finally, ΔE(Solv) (or ΔG) changes slowly near the minimum with variations of NW, and thus, the predicted number of water molecules in a unit cell can easily be somewhat off. Indeed, there can be a statistical distribution of NW values for the unit cells. This manifold of values brings about a multiminima problem discussed elsewhere.[14] For this reason we located the global minimum for each simulation by carefully choosing many different

(11) G. C. Lie and E. Clementi, *J. Chem. Phys.*, 2195, (1975); G. C. Lie, E. Clementi, and M. Yoshimine, *J. Chem. Phys.*, **64**, 314 (1976).

(12) See, for example, the five volumes "Water: A Comprehensive Treastise", F. Franks, Ed., Plenum Press, New York, 1973.

(13) S. F. Boys and F. Bernardi, *Mol. Phys.*, **19**, 558 (1970); W. Kolos, *Theor. Chim. Acta*, **51**, 219 (1979); A. Johansson, P. Kollman, and S. Rothenberg, *Theor. Chim. Acta*, **29**, 173 (1973).

(14) K. S. Kim and E. Clementi the IBM IS & TG, POK-36 (1984); K. S. Kim and E. Clementi, to be published.

initial samples. This procedure gives a reasonable assurance that we have located the absolute minimum.

Acknowledgment. K.S.K. would like to thank the National Foundation for Cancer Research (NFCR) for financial support. We would also like to acknowledge Dr. S. Chin for reviewing the manuscript.

Registry No. Proflavine complex with deoxy(cytidylyl-3,5'-guanosine), 73113-31-2.

Inactivation of Cytochrome P-450 by a Catalytically Generated Cyclobutadiene Species

Ralph A. Stearns and Paul R. Ortiz de Montellano*

Contribution from the Department of Pharmaceutical Chemistry, School of Pharmacy and Liver Center, University of California, San Francisco, California 94143. *Received May 24, 1984*

Abstract: 2,3-Bis(carbethoxy)-2,3-diazabicyclo[2.2.0]hex-5-ene (DDBCH), synthesized by a route analogous to that reported for the preparation of the bis(carbomethoxy) analogue, inactivates the phenobarbital-inducible cytochrome P-450 isozymes of rat liver in a time-, NADPH-, and oxygen-dependent manner. The enzymes are protected by carbon monoxide and competitive alternative substrates but not by glutathione. The cyclobutenyl π bond and the diazabicyclo[2.2.0] skeleton are required for destructive activity, but hydrolytic removal of the carbamate groups is not. Enzyme inactivation reflects alkylation of the prosthetic heme group of the enzyme by a catalytically generated reactive species. The alkylated prosthetic group has been isolated and has been characterized, after demetallation and esterification, as *N*-(2-cyclobutenyl)protoporphyrin IX. The *N*-alkyl group is primarily located on the nitrogen of pyrrole ring D. DDBCH is thus oxidized by cytochrome P-450 to a cyclobutadienoid species that alkylates the prosthetic heme group.

The inactivation of cytochrome P-450 enzymes by catalytically activated substrates is of toxicological, pharmacological, and mechanistic importance. The inactivation of cytochrome P-450 enzymes can alter patterns of metabolism, perturb heme and hemoprotein synthesis, and, in some instances, inhibit critical cellular processes.[1] The sedative hypnotics ethchlorvynol and novonal, for example, alkylate the prosthetic heme groups of cytochrome P-450 enzymes in a process that initiates uncontrolled porphyrin synthesis and causes, or exacerbates, the clinical symptoms of porphyria in genetically predisposed patients.[2-4] In contrast, the *highly specific* inhibition of individual cytochrome P-450 isozymes is a promising route to the design of drugs and other pharmacologically active agents. Two such agents now in use are miconazole, an antimycotic drug that inhibits the 14-demethylation of ergosterol in fungi,[5] and piperonyl butoxide, an insecticide synergist.[6] Finally, in a mechanistic context, suicide substrates have been employed by this laboratory to explore the electronic nature of the catalytic mechanisms and the topologies of the active sites of cytochrome P-450 enzymes.[7,8]

The construction of isozyme-specific suicide substrates depends on the availability of latent destructive functionalities that can be incorporated into substrates recognized by the target enzymes. We have established in earlier work that introduction of a terminal carbon-carbon double or triple bond into a substate conveys cytochrome P-450 destructive activity.[1,7] We have recently, in a departure from the electrophilic and radical species on which most suicide substrates are based, established that 1-aminobenzotriazole is catalyticaly oxidized to benzyne or a closely related

Scheme I. Synthesis of DDBCH

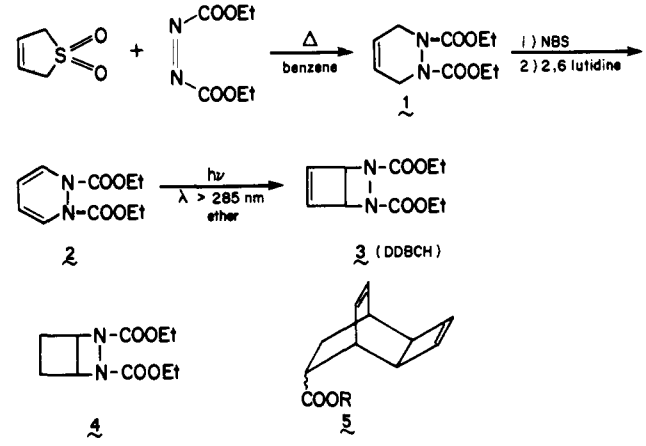

species and that this species inactivates cytochrome P-450 enzymes in animals, plants, and insects with exceptional efficiency.[9-12] The high activity and surprisingly low toxicity of this benzyne precursor led us to search for alternative stereoelectronically activated moieties that could be unmasked by the catalytic action of redox enzymes. We report here that cytochrome P-450-catalyzed oxidation of 2,3-bis(carbethoxy)-2,3-diazabicyclo[2.2.0]hex-5-ene (DDBCH) unveils a highly antiaromatic and reactive cyclobutadienoid moiety that efficiently alkylates the prosthetic heme group of the enzyme.

Results

Synthesis. 2,3-Biscarbethoxy-2,3-diazabicyclo[2.2.0]hex-5-ene (DDBCH) was synthesized from butadiene and ethyl azodicarboxylate by the sequence outlined in Scheme I. The individual steps in the sequence were adopted in modified form from liter-

(1) Ortiz de Montellano, P. R.; Correia, M. A. *Annu. Rev. Pharmacol. Toxicol.* **1983**, *23*, 481-503.
(2) Ortiz de Montellano, P. R.; Bellan, H. S.; Mathews, J. M. *J. Med. Chem.* **1982**, *25*, 1174-1179.
(3) Ortiz de Montellano, P. R.; Stearns, R. A.; Langry, K. C. *Molec. Pharmacol.* **1984**, *25*, 310-317.
(4) Moore, M. R. *Int. J. Biochem.* **1980**, *12*, 1089-1097.
(5) Beggs, W. H.; Andrews, F. A.; Sarosi, G. A. *Life Sci.* **1981**, *28*, 111-118.
(6) Hodgson, E.; Philpot, R. M. *Drug. Metab. Rev.* **1974**, *3*, 231-301.
(7) Ortiz de Montellano, P. R. "Review in Biochemical Toxicology"; Hodgson, E., Bend, J. R., Philpot, R. M., Eds.; Elsevier: New York, 1984; pp 1-26.
(8) Ortiz de Montellano, P. R. In "Bioactivation of Foreign Compounds"; Anders, M. W., Ed.; Academic Press: New York, 1985; pp 121-155.
(9) Ortiz de Montellano, P. R.; Mathews, J. M. *Biochem. J.* **1981**, *195*, 761-764.
(10) Reichhhart, D.; Simon, A.; Durst, F.; Mathews, J. M.; Ortiz de Montellano, P. R. *Arch. Biochem. Biophys.* **1982**, *216*, 522-529.
(11) Ortiz de Montellano, P. R.; Mathews, J. M.; Langry, K. C. *Tetrahedron* **1984**, *40*, 511-519.
(12) Bally, T.; Masamune, S. *Tetrahedron* **1980**, *36*, 343-370.

0002-7863/85/1507-0234$01.50/0